Solute Transport Model with Cation Exchange under Redox Environment and its Application for Designing the Slow Infiltration Set-up

GINGGING GUERRA
Graduate Student, Institute of Environmental Systems, Kyushu University, Fukuoka City, Japan

KENJI JINNO
Professor, Institute of Environmental Systems, Kyushu University, Fukuoka City, Japan

YOSHINARI HIROSHIRO
Associate Professor, Institute of Environmental Systems, Kyushu University, Fukuoka City, Japan

KOJI NAKAMURA
Graduate Student, Institute of Environmental Systems, Kyushu University, Fukuoka City, Japan

ABSTRACT: The present trend of disposing treated sewage water by allowing it to infiltrate the soil brings a new dimension to environmental problems. It is therefore necessary to identify the chemicals likely to be present in treated sewage water. A soil column experiment was conducted to determine the behavior of chemical species in soil columns applied with secondary treated sewage water. To predict the behavior of chemical species, a multicomponent solute transport model that includes the biochemical redox process and cation exchange process was developed. The model computes changes in concentration over time caused by the processes of advection, dispersion, biochemical reactions and cation exchange reactions. The solute transport model was able to predict the behavior of the different chemical species. The model reproduced the sequential reduction reaction. To design the safe depth of plow layer where NO_3^- is totally reduced, a numerical study of NO_3^- leach was done and it was found out that the pore velocity and concentration of CH_2O at the inject water was found to affect NO_3^- reduction in the mobile pore water phase. It is revealed that the multicomponent solute transport model is useful to design the land treatment system for NO_3^- removal from wastewater.

1 INTRODUCTION

The concept of deriving beneficial uses from treated wastewater coupled with increasing pressures on water resources has prompted the emergence of wastewater reclamation, recycling and reuse as integral components of water resource management. Land application of wastewater is a simple low cost system for treatment of sewage and has been in practice in many parts of the world because it is believed that passage through the soil environment of wastewater will provide further removal of certain chemical and microbial contaminants. However, the present trend of disposing treated sewage water by allowing it to infiltrate the soil brings a new dimension to environmental problems. Nitrogen from such treatment systems is currently of concern because of the nitrate contamination of drinking water supplies and the eutrophication of coastal waters. Therefore it is necessary to study the governing mechanisms for the transport and fate of nitrogen and other contaminants from treated sewage water. The development and use of mathematical models provides a better understanding of the important biological, chemical and hydrological processes relevant to contaminant transport.

For simulating nitrogen transport and transformations, nitrification and denitrification in groundwater must be represented by kinetic expressions, which take the form of multiple nutrient Monod type equations (Kinzelbach et al., 1991). Several groups of researchers have recently simulated heterotrophic denitrification in one- or two- dimensional saturated groundwater flow systems. Kinzelbach et al. was able to describe the interactive transport of oxygen, nitrate, organic substrates and microbial mass in two dimensions, including the possibility of diffusion-limited exchange between different phases in the aquifer. Lensing et al. used a multicomponent transport reaction model to bacterially catalyzed redox processes. The exchange between the three different phases: pore water phase, bio phase and aquifer matrix is considered. The sub-models are coupled with the equations of the microbially mediated redox reactions. Mac Quarie et al. have presented the theory and numerical solution of a reactive transport model that is intended to represent the major flow, transport and

biogeochemical processes involved in wastewater migration in a shallow aquifer. A numerical model was developed for variably saturated flow and reactive transport of multiple species. The model suggested that adding labile organic carbon sources to septic drain fields could enhance heterotrophic denitrification and thus reduce NO_3^- concentration in shallow ground water. The simulations could help to clarify the effect of the ways of organic matter application on the process of denitrification.

To assess and predict the behavior of different chemical species in soil columns applied with secondary treated sewage water. A solute transport model that takes into consideration the biochemical reactions and cation exchange reactions was developed. The results of the soil column experiments were compared with the results of simulation model. It was found out that the multicomponent solute transport model was able to predict the behavior of different chemical species in the soil column applied with secondary treated sewage water, however it is necessary to determine the safe depth of the plow layer that is safe for nitrate (NO_3^-) leaching.

The objective of this study is to design the slow rate infiltration setup for nitrate removal from treated sewage water using the multicomponent solute transport model. Slow rate treatment occurs by means of physical, chemical and biological processes at the surface and as the wastewater flow through the plant-soil matrix. The numerical modeling of NO_3^- leach was done using the multicomponent solute transport model to determine the effect of the pore velocity and input CH_2O concentration needed to reduce the NO_3^- concentration. To design the depth of the plow layer that is safe for NO_3^- leaching, it is necessary to determine the depth where NO_3^- will be totally reduced. In the simulation model the input values of pore velocity and input CH_2O concentration was varied to design the safe depth of plow layer in soil columns. It was found out that the pore velocity and concentration of CH_2O at the inject water was found to affect NO_3^- reduction in the mobile pore water phase. It is revealed that the multicomponent solute transport model is useful to design the land treatment system for NO_3^- removal from secondary treated wastewater.

2 EXPERIMENTAL APPARATUS AND PROCEDURE

The soil column experiment was conducted using soils collected from actual paddy field and were packed in 10 cm diameter PVC cylinder column with 10 cm and 20 cm thickness of plow layers respectively (Fig.1). Table 1 shows the soil properties of the paddy soil and Table 2 shows the chemical component of the paddy soil. Secondary treated sewage water was constantly supplied up to 5 cm at the top of the soil columns in order to reproduce the redox condition similar to paddy field. Glass beads were used to support the plow layer in soil column. Table 3 shows the concentration of the injection water. The experiment was conducted for the duration of 49 days and the average temperature was measured at 30^{o}C. Soil solution samples collected by porous cup and column outflow were analyzed for Na^+, K^+, Mg^{2+}, Ca^{2+}, Mn^{2+}, Fe^{2+}, NH_4^+-N and NO_3^- -N concentrations. EC (Electrical Conductivity), pH and ORP (Oxidation Reduction Potential) were also measured.

Table 1. Soil properties of the paddy soil

Cation exchange capacity	**Selectivity coefficients**			
CEC (mmolc/100g)	$K_{Ca/Na}$	$K_{Ca/K}$	$K_{Ca/Mg}$	$K_{Ca/Fe}$
13.52	0.453	0.0428	1.2	1.2

Table 2. Chemical component of the paddy soil

Chemical Species	**% composition**
Fe_2O_3	5.34
MnO_2	0.05
Al_2O_3	8.09
SiO_2	77.58
CH_2O	6.08
C	1.96
H	0.76
N	0.15
Total	100.01

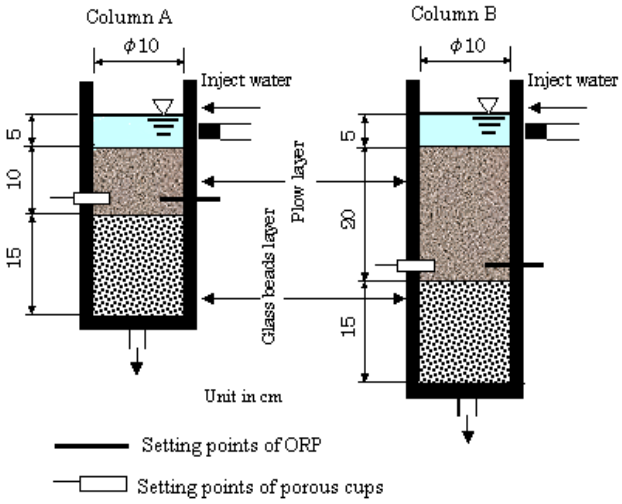

Table 3. Concentration of injection water

Na^+	10.146 meq/L	NH_4^+	0.432 meq/L
K^+	0.775 meq/L	NO_3^-	0.378 meq/L
Ca^{2+}	4.164 meq/L	TOC	6.23 meq/L
Mg^{2+}	2.085 meq/L	EC	1.55 mS/cm
Fe^{2+}	0.066 meq/L	pH	7.2
Mn	0.024 meq/L	Temperature	30°C

Fig. 1. Experimental column equipment

3 MULTICOMPONENT SOLUTE TRANSPORT MODEL

The biochemical and chemical model (Fig. 2) describe the interaction of O_2, NO_3^-, CH_2O, bacteria, MnO_2, $Fe(OH)_3$, Na^+, K^+, Mg^{2+},Ca^{2+}, $Mn^{2+}$and Fe^{2+}. This model takes into account the microbially mediated redox reaction and the cation exchange reaction. It also takes into consideration the four different phases: mobile pore water phase, immobile biophase, solid phase and solid matrix phase. The bacteria are assumed to reside in an immobile biophase. Exchange processes are considered between the different phases.

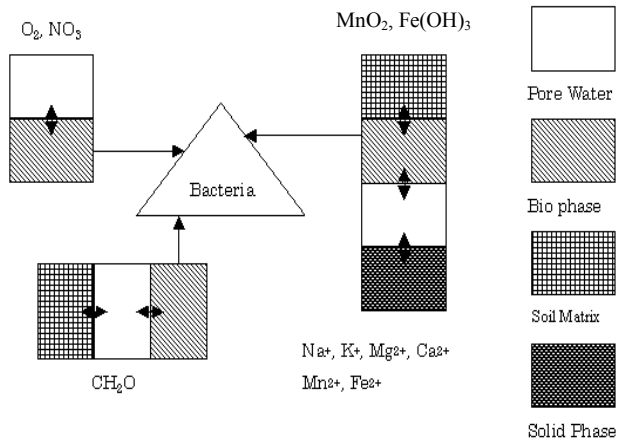

Fig. 2. Scheme of biochemical model

4 REACTIVE SOLUTE TRANSPORT MODEL

The one-dimensional partial differential equation governing the convective-dispersive solute transport of chemical species *i* considering biochemical and chemical reactions in a sub-aqueous soil can be written as (Bear, 1972; Kinzelbach et al., 1991; Lensing et al., 1994; Hiroshiro et al., 1999):

$$\frac{\partial}{\partial t}\left(\theta_w [C_i]_{mob}\right)+\frac{\partial}{\partial x}\left(\theta_w v' [C_i]_{mob}\right)=\frac{\partial}{\partial x}\left(\theta_w D \frac{\partial [C_i]_{mob}}{\partial x}\right)+\theta_w S1_{(i)}+\theta_w S2_{(i)}+\theta_w S3_{(i)} \quad (1)$$

where $i=1,2,...,N$, C_i is the concentration of chemical species i in the pore water (mmol l^{-1}), v' is pore water velocity (cm sec^{-1}), t is time (sec), x is distance, D is the hydrodynamic dispersion coefficient (cm^2 sec^{-1}), N is 9 and the chemical species given by i= 1,2,3,4,5,6,7,8, and 9 correspond to Na^+, K^+, Mg^{2+}, Ca^{2+}, Mn^{2+}, Fe^{2+}, O_2, NO_3^- and CH_2O, respectively. $S1_{(i)}$ $S2_{(i)}$ and $S3_{(i)}$ are the chemical sink/source term representing the exchange with other phases and the chemical and biochemical reactions (mmol $l^{-1}sec^{-1}$) and formulated as follows:

$$\theta_w S1_{(i)}=\frac{\alpha\theta_{bio}\theta_w}{\theta_{bio}+\theta_w}\left([C_i]_{bio}-[C_i]_{mob}\right) \quad (2)$$

$$\theta_w S2_{(i)}=\frac{\beta\theta_{mat}\theta_w}{\theta_{mat}+\theta_w}\left([C_i]_{mat}-[C_i]_{mob}\right) \quad (3)$$

$$\theta_w S3_{(i)}=-\frac{\partial}{\partial t}\left(\theta_w [C_i]_{im}\right) \quad (4)$$

where $S1_{(i)}$ is the exchange reaction term at the concentration difference between the pore water and the biophase, $S2_{(i)}$ is the exchange reaction term at the concentration difference between pore water and the soil matrix, and $S3_{(i)}$ is the cation exchange reaction term between the pore water and the solid phase. $[C_i]_{mob}$, $[C_i]_{bio}$, $[C_i]_{mat}$ and $[C_i]_{im}$ correspond to the concentration of chemical species (mmol l^{-1}) in the pore water, the biophase, the soil matrix, and the solid phase, respectively. α and β are the exchange coefficients. In equations (2) and (3) the theory of mass transport at the boundary of film interface is applied. The biophase is conceptualized as an operative means to easily include diffusion limited exchange process between the mobile pore water and bacteria. The diffusion limitation can be due either to microscale (or real biofilm) diffusion or to limited macroscale exchange between different zones of the aquifer. This diffusional transfer can be represented by mass transport exchange coefficients, α and β. (Kinzelbach et al, 1991). The chemical species considered in the model are summarized in Table 4.

Table 4. Chemical species considered in the model

Pore water	Na^+_{mob}	Ca^{2+}_{mob}	Mg^{2+}_{mob}	K^+_{mob}	Mn^{2+}_{mob}	Fe^{2+}_{mob}	$O_{2\,mob}$	$NO_3^-{}_{mob}$	CH_2O
Bio phase	$O_{2\,bio}$	$NO_3^-{}_{bio}$	$Mn^{2+}{}_{bio}$	Fe^{2+}_{bio}	CH_2O_{bio}	$MnO_{2\,bio}$			
Solid phase	Na^+_{im}	Ca^{2+}_{im}	K^+_{im}	Mg^{2+}_{im}	Mn^{2+}_{im}	Fe^{2+}_{im}			
Soil matrix	CH_2O_{mat}	MnO_{2mat}	$Fe(OH)_{3mat}$						
Bacteria	X1	X2	X3						

For the chemical species related to Fe^{2+} the following equations are formulated:

Biophase:

$$Fe^{2+}:\frac{\partial}{\partial t}(\theta_{bio}[Fe^{2+}]_{bio})=\frac{\theta_{bio}}{P_{Fe^{2+}}}\left[\frac{\partial X3}{\partial t}\right]_{Iron}-\frac{\alpha\theta_{bio}\theta_w}{\theta_{bio}+\theta_w}\left([Fe^{2+}]_{bio}-[Fe^{2+}]_{mob}\right) \quad (5)$$

$$Fe(OH)_3:\frac{\partial}{\partial t}(\theta_{bio}[Fe(OH)_3]_{bio})=-\frac{\theta_{bio}}{U_{Fe(OH)_3}}\left[\frac{\partial X3}{\partial t}\right]_{grow}-\frac{\gamma\theta_{bio}\theta_{mat}}{\theta_{bio}+\theta_{mat}}\left([Fe(OH)_3]_{bio}-[Fe(OH)_3]_{mat}\right) \quad (6)$$

Pore water phase:

$$Fe^{2+}:\frac{\partial}{\partial t}(\theta_w[Fe^{2+}]_{mob})+\frac{\partial}{\partial x}(\theta_w v'[Fe^{2+}]_{mob})=\frac{\partial}{\partial x}(\theta_w D\frac{\partial[Fe^{2+}]_{mob}}{\partial x})+\frac{\alpha\theta_{bio}\theta_w}{\theta_{bio}+\theta_w}\left([Fe^{2+}]_{bio}-[Fe^{2+}]_{mob}\right)+\theta_w S3_{Fe} \quad (7)$$

Solid Phase:

$$Fe^{2+}:\frac{\partial}{\partial t}(\theta_w[Fe^{2+}]_{im})=-\theta_w S3_{Fe^{2+}} \quad (8)$$

Soil Matrix:

$$Fe(OH)_3:\frac{\partial}{\partial t}(\theta_{mat}[Fe(OH)_3]_{mat})=\frac{\gamma\theta_{bio}\theta_{mat}}{\theta_{bio}+\theta_{mat}}\left([Fe(OH)_3]_{bio}-[Fe(OH)_3]_{mat}\right) \quad (9)$$

Bacteria:

$$X3:\left[\frac{\partial X3}{\partial t}\right]_{Total\_Growth}=\left[\frac{\partial X3}{\partial t}\right]_{grow}+\left[\frac{\partial X3}{\partial t}\right]_{decay} \tag{10}$$

$$X3:\left[\frac{\partial X3}{\partial t}\right]_{grow}=v_{\max}^{Fe(OH)_3}\cdot\frac{IC_{NO_3^-}}{IC_{NO_3^-}+[NO_3^-]_{bio}}\cdot\frac{[CH_2O]_{bio}}{K_{CH_2O}+[CH_2O]_{bio}}\cdot\frac{[Fe(OH)_3]_{bio}}{K_{Fe(OH)_3}+[Fe(OH)_3]_{bio}}\cdot X3 \tag{11}$$

$$\left[\frac{\partial X3}{\partial t}\right]_{decay}=-v_{X3dec}\cdot X3 \tag{12}$$

where α, γ are the exchange coefficients, θ_{bio}, θ_w, and θ_{mat} correspond to water content for bio phase, mobile phase and matrix phase respectively, $P_{Fe^{2+}}$ is the production factor for Fe^{2+}, $U_{Fe(OH)_3}$ is the growth yield factor for $Fe(OH)_3$, $S3_{Fe^{2+}}$ is the pore water and solid phase exchange reaction term of Fe^{2+}, $IC_{NO_3^-}$ is the inhibition concentration of NO_3^- against O_2, K_{CH_2O} is the half velocity concentration for CH_2O, $v_{\max}^{Fe(OH)_3}$ is the maximum growth rate of bacteria X3 and v_{X3dec} is the constant decay rate of bacteria X3.

5 BACTERIA GROWTH

The modeling of sequential redox sequences requires the consideration of different metabolisms. Bacteria X1, X2 and X3 that are assumed to reside in the immobile biophase are considered in the model. Under aerobic conditions bacteria X1 uses O_2 as electron acceptor while under anaerobic conditions. NO_3^- is used as electron acceptor. Bacteria X2 uses MnO_2 while bacteria X3 uses $Fe(OH)_3$ as electron acceptor. These bacteria use dissolved organic carbon (CH_2O) as carbon source and oxidize this substrate to CO_2 in the model. The growth of different groups of microbial populations in the biophase is based on Monod kinetics and are formulated as follows:

$$X1:\left[\frac{\partial X1}{\partial t}\right]_{Total\_Growth}=\left[\frac{\partial X1}{\partial t}\right]_{aerobic\_condition}+\left[\frac{\partial X1}{\partial t}\right]_{denitrifying\_condition}+\left[\frac{\partial X1}{\partial t}\right]_{decay} \tag{13}$$

$$\left[\frac{\partial X1}{\partial t}\right]_{aerobic\_condition}=v_{\max}^{O_2}\cdot\{1-F(O_{2bio})\}\cdot\frac{[CH_2O]_{bio}}{K_{CH_2O}+[CH_2O]_{bio}}\cdot\frac{[O_2]_{bio}}{K_{O_2}+[O_2]_{bio}}\cdot X1 \tag{14}$$

$$\left[\frac{\partial X1}{\partial t}\right]_{denitrifying\_condition}=v_{\max}^{NO_3^-}\cdot\{F(O_{2bio})\}\cdot\frac{[CH_2O]_{bio}}{K_{CH_2O}+[CH_2O]_{bio}}\cdot\frac{[NO_3^-]_{bio}}{K_{NO_3^-}+[NO_3^-]_{bio}}\cdot X1 \tag{15}$$

$$\left[\frac{\partial X1}{\partial t}\right]_{decay}=-v_{X1dec}\cdot X1 \tag{16}$$

$$X2:\left[\frac{\partial X2}{\partial t}\right]_{grow}=v_{\max}^{MnO_2}\cdot\frac{IC_{NO_3^-}}{IC_{NO_3^-}+[NO_3^-]_{bio}}\cdot\frac{[CH_2O]_{bio}}{K_{CH_2O}+[CH_2O]_{bio}}\cdot\frac{[MnO_2]_{bio}}{K_{MnO_2}+[MnO_2]_{bio}}\cdot X2 \tag{17}$$

$$\left[\frac{\partial X2}{\partial t}\right]_{decay}=-v_{X2dec}\cdot X2 \tag{18}$$

$$X3:\left[\frac{\partial X3}{\partial t}\right]_{Total\_Growth}=\left[\frac{\partial X3}{\partial t}\right]_{grow}+\left[\frac{\partial X3}{\partial t}\right]_{decay} \tag{19}$$

$$X3:\left[\frac{\partial X3}{\partial t}\right]_{grow}=v_{\max}^{Fe(OH)_3}\cdot\frac{IC_{NO_3^-}}{IC_{NO_3^-}+[NO_3^-]_{bio}}\cdot\frac{[CH_2O]_{bio}}{K_{CH_2O}+[CH_2O]_{bio}}\cdot\frac{[Fe(OH)_3]_{bio}}{K_{Fe(OH)_3}+[Fe(OH)_3]_{bio}}\cdot X3 \tag{20}$$

$$\left[\frac{\partial X3}{\partial t}\right]_{decay}=-v_{X3dec}\cdot X3 \tag{21}$$

$$F(O_{2bio})=0.5-\frac{1}{\pi}\tan^{-1}[(O_{2bio}-O_{2thres})xf_{sl}] \tag{22}$$

where X1, X2 and X3 correspond to the concentration of O_2 and NO_3^-, MnO_2 and $Fe(OH)_3$ reducing bacteria, $v_{\max}^{O_2}$, $v_{\max}^{NO3-}$, $v_{\max}^{MnO2}$ and $v_{\max}^{Fe(OH)3}$ correspond to the maximum growth rate of O_2, NO_3^-, MnO_2 and $Fe(OH)_3$ reducing bacteria, v_{X1dec}, v_{X2dec} and v_{X3dec} correspond to the constant decay rate of bacteria X1, X2 and X3, $F(O_{2bio})$ is the switching function parameter, O_{2thres} is the threshold concentration of O_2, f_{sl} is the slope of switch function, $[O_2]_{bio}$, $[NO_3^-]_{bio}$ and $[CH_2O]_{bio}$ correspond to concentration of O_2, NO_3^- and CH_2O in the bio phase. K_{O_2}, $K_{NO_3^-}$ and K_{CH_2O} correspond to half velocity concentration of O_2, NO_3^- and CH_2O in the bio phase.

The bacteria are assumed to consume dissolved oxygen (DO) as long as it is available and then switch to nitrate as electron acceptor. The switching between aerobic and denitrifying growth conditions is based on the assumption of a non-competitive inhibition and is realized by a weighting function $F(O_{2bio})$ dependent on the oxygen concentration, which was developed and tested by Kinzelbach, et al. (1991). Equation (22) is based on the assumption that the same microorganisms are capable of either aerobic or denitrifying growth, depending on the oxygen concentration in their nearby environment. It allows adjustment of two characteristic features of the microbial switching, the slope f_{sl} and the threshold concentration of oxygen O_{2thres}, according to laboratory or field measurements. It is also assumed that the functional bacterial group X1 reduces nitrate quantitatively to N_2 under anaerobic conditions. This biochemical model is mathematically similar to other models that use Monod type kinetics to describe microbial activity (e.g. Schäfer et al., 1998; Kinzelbach et al., 1991).

6 MODELLING METHODOLOGY

The one-dimensional solute transport equation is solved for each chemical species. The model couples the flow equation with the solute-transport equation. The flow and transport equation are discretized using a rectangular, uniformly spaced, block centered, finite difference grid. Since artificial oscillation and numerical dispersion are encountered in the finite difference method when applied to advection-dominated problem, the method of characteristics (MOC) was used to eliminate numerical dispersion (Zheng and Bennett, 1995). The iterative numerical procedure employed for coupling of physical transport and chemical processes was based on Momii et al. (1997). The multicomponent solute transport model is applicable for one-dimensional problem involving steady-state flow. The model computes changes in concentration over time caused by the processes of advection, dispersion, cation exchange reactions and biochemical reactions.

7 PARAMETER ESTIMATION

The modelling of multicomponent solute transport with biochemical reaction processes is complex because it involves specification of many biochemical parameters. Monod kinetic parameters for heterotrophic processes were selected following a review of several studies related to wastewater treatment modeling and simulation of denitrification in groundwater (Kinzelbach et al, 1991; Lensing et al, 1994; Schäfer et al, 1998; Hiroshiro et al, 1999). In general these parameters are affected by temperature. The temperature effect on the denitrification rate is an important feature in the design of denitrification process. Carrerra et al. (2003) studied the influence of temperature on denitrification of an industrial high-strength nitrogen wastewater in a two-sludge system and found out that the maximum denitrification rate is much higher at 25°C. The most favorable temperature for denitrification ranges from 20°C to 30°C and the average temperature measured in the present experiment is high enough at 30°C. Consequently, the parameters adjusted for this particular simulation may be the case for the most desirable denitrification. In this study, the maximum growth rate of bacteria X1, $v_{\max}^{O_2}$ and $v_{\max}^{NO_3^-}$ was calibrated by trial and error method until the O_2 and NO_3^- in the simulation model fit the measured concentration of O_2 and NO_3^-.

8 RESULTS AND DISCUSSIONS

8.1 Flow rate and Permeability

Fig. 3 shows the flow rate in Column A and Column B are rapidly decreasing during the first ten days and then after ten days the flow rate in Column A is almost the same with the flow rate in Column B. The average velocity was obtained by dividing the flow rate by the surface area of the column. It was assumed that the steady state was attained at the flow rate of 40 ml/day. Then the pore water velocity was determined by dividing the

average velocity by porosity. In the simulation model the pore water velocity was assumed constant (VK=7.68x10^{-6} cm/sec) since the model considered only the reduced layer that is saturated. Fig. 4 shows the permeability in Column A and Column B are rapidly decreasing during the first two days and then after ten days the permeability in Column A is almost the same with the permeability in Column B. The rapid decrease in permeability could be due to clogging of the soil pores as a result of the growth of bacteria. From the experimental results of flow rate and permeability, there is no significant difference between Column A and Column B. Similar results can be expected with the two soil columns.

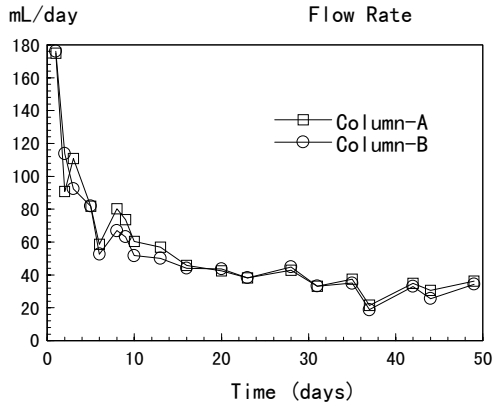

Fig. 3 Flow rate in Columns A and B

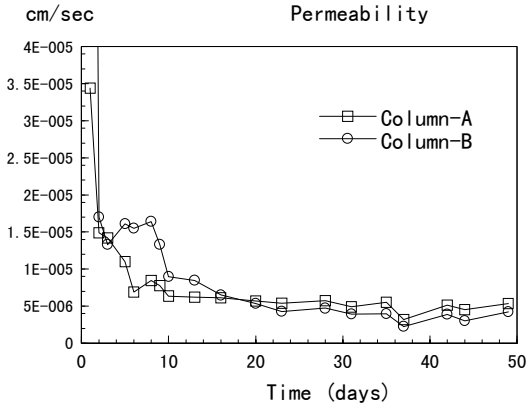

Fig. 4 Permeability in Columns A and B

8.2 Simulation result of Dissolved Oxygen, NO_3^- and CH_2O

Fig. 3 shows the simulation result of DO, NO_3^- and CH_2O concentration at the top 5 cm of plow layer in the mobile phase at the early stage. DO concentration reduced at the top 0.5 cm of the column where DO concentration decreased to zero after 30 hours. Denitrification occurred immediately at the top 0.5 cm of the column where NO_3^- concentration was reduced to zero after 31 hours, following the reduction of DO. CH_2O concentration decreased only at the top 2 cm of the column and then increased near to original concentration. CH_2O concentration degradation is relatively fast at the top 2 cm of the column, where O_2 concentration is readily available. On the other hand, CH_2O degradation is very slow at the deeper downstream of the column where both O_2 and NO_3^- concentration are very small.

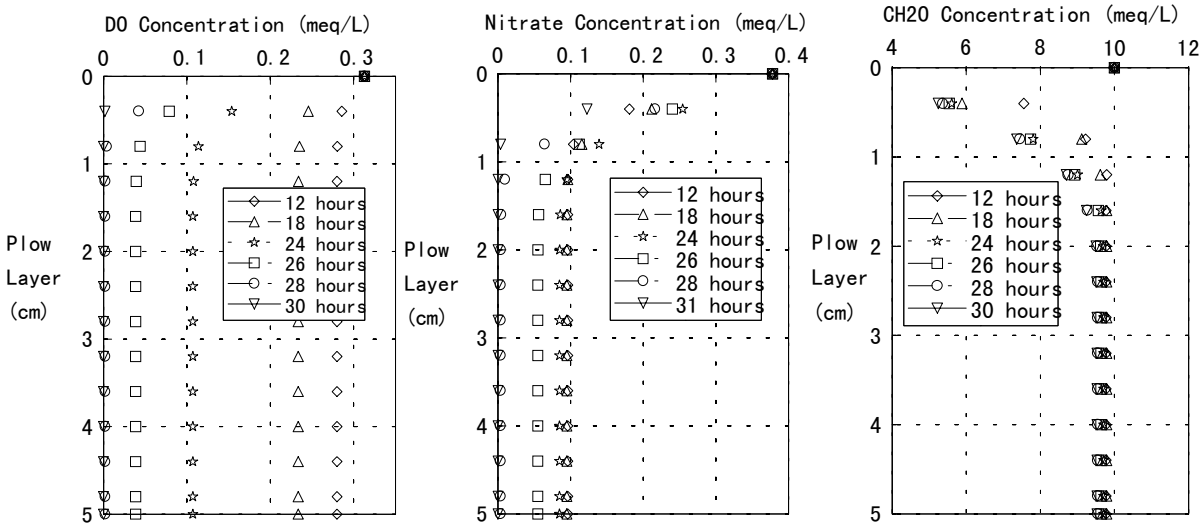

Fig. 3. Simulation result of Dissolved Oxygen, NO_3^- and CH_2O

8.3 Comparison of observed and calculated concentration in the mobile phase

The multicomponent solute transport model was tested by comparing the simulation results with the results of the soil column experiment by using the concentration of inject water from the soil column experiment (Table 1) as the concentration of inject water in the simulation model. It was found out that the multicomponent solute transport model was able to predict the behavior of different chemical species in the soil column applied with secondary treated sewage water. Fig. 4 shows the observed cation concentration correlated fairly well with the calculated cation concentrations. K^+ concentration showed almost constant values. Na^+ concentration decreased while $Ca^{2+}$and Mg^{2+} concentrations increased at the depth 17 cm and depth 20 cm of the column due to desorption of Ca^{2+} and Mg^{2+} by Mn^{2+} and Fe^{2+}. Fig 5 shows the comparison of observed and calculated concentrations of NO_3^-, Mn^{2+} and Fe^{2+}. NO_3^- concentration rapidly decreased at the depth 17 cm due to denitrification while Mn^{2+} and Fe^{2+} concentration increased due to dissolution from MnO_2 and $Fe(OH)_3$ during infiltration through the plow layer. These changes in concentration indicated that chemical reactions had occurred in all parts of the column.

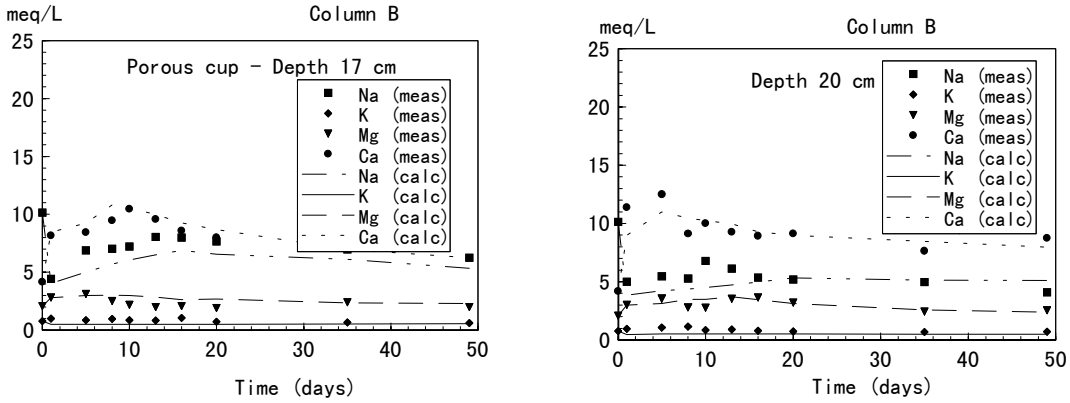

Fig. 4. Comparison of observed and calculated cation concentration in the mobile phase

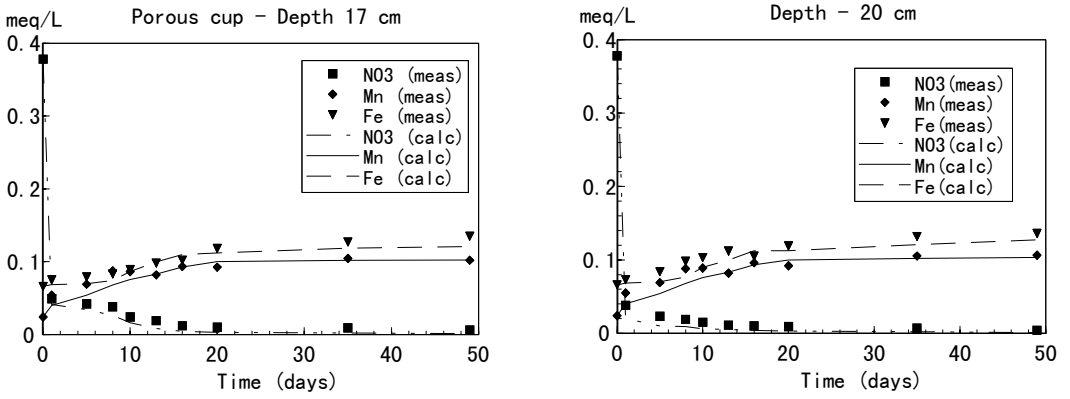

Fig. 5. Comparison of observed and calculated NO_3^-, Mn^{2+} and Fe^{2+} concentration in the mobile phase

8.4 Simulation result of CH_2O, MnO_2 , $Fe(OH)_3$ and Bacteria concentration in the biophase

Fig. 6 shows the simulation results of the temporal variation of CH_2O, MnO_2 and $Fe(OH)_3$ in the biophase. CH_2O concentration decreased during the first 5 days while MnO_2 and $Fe(OH)_3$ decreased after 5 days due to consumption of bacteria. Fig. 7 shows the simulation results of the temporal variation of X1, X2 and X3 bacteria concentration at different depths in the biophase. The maximum growth of bacteria X1 occurred at the depth 5 cm of the column, where high concentrations of O_2, NO_3^- and CH_2O are present. Bacteria X1 increases rapidly during the first 5 days due to presence of O_2, NO_3^- and CH_2O concentration at the top 5 cm of the column then

decreases rapidly due to decreased O_2 and NO_3^-. Bacteria X2 and X3 increase after 5 days and then decrease gradually. Bacteria X3 increases higher than bacteria X2 due to higher concentration of $Fe(OH)_3$ than MnO_2 in the matrix phase and consequently in the biophase.

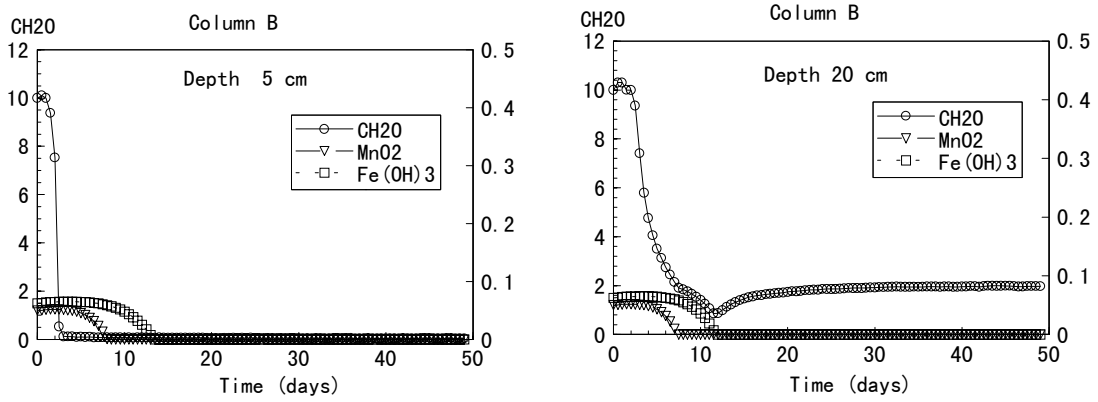

Fig. 6. Temporal variation of CH_2O, MnO_2 and $Fe(OH)_3$ concentration at different depths in the bio phase

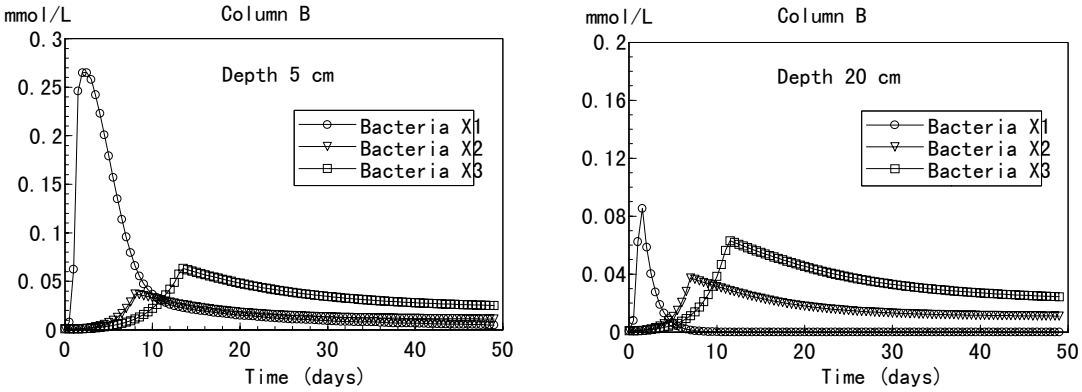

Fig. 7. Temporal variation of bacteria concentration at different depths in the bio phase

The result of the solute transport model produced interesting observations on the behavior of the different chemical species present in the soil columns applied with secondary treated sewage water. The result of the numerical simulation approximately agreed with the experimental results.

9 DESIGN OF INFILTRATION TREATMENT

In order to design the thickness of plow layer that is safe for nitrate leaching, it is necessary to determine the depth where denitrification occurs. Denitrification has been inferred from the observation of decreasing NO_3^- concentration and corresponding decline in dissolved oxygen concentration. Reduction of NO_3^- to N_2 by organic matter under anoxic conditions as a result of denitrification in soils is well documented. A number of studies shown that reduction of NO_3^- by organic matter oxidation can be important in aquifers. Accordingly Kinzelbach and Schaefer (1989) model NO_3^- reduction by organic matter in a sandy aquifer using the kinetic approach and found that the field data are well described by reaction of NO_3^- with degradable organic matter in sediments.

The design of infiltration treatment is also primarily affected by the application rate. In rapid infiltration systems, the required treatment performance is of primary importance in determining the application rate. Lance and Gerba (1977) showed that decreasing the application rate from the hydraulic limit could result in increased removals of constituents, especially NO_3^-. Since the chief mechanism of NO_3^- removal in rapid infiltration systems is denitrification and denitrification requires adequate detention time, anoxic conditions and adequate organic carbon to drive the reaction. The reduction in application rate increases detention time and increases the

potential for denitrification. The design of slow rate infiltration treatment considered the effects of pore velocity and input CH_2O concentration. In designing the depth of the plow layer that is safe for NO_3^- leaching, it is necessary to determine the depth where NO_3^- will be totally reduced. In the simulation model the input values of pore velocity and input CH_2O concentration was varied to design the safe depth of plow layer in soil columns. The design of the thickness of plow layer is important in land treatment system design and operation, so as to maximize land treatment efficiency and minimize operation and maintenance costs.

9.1 Effect of pore velocity VK on NO_3^- leaching

It was assumed that the steady state was attained at the flow rate of 40 ml/day. Then the pore water velocity was determined by dividing the average velocity by porosity. In the simulation model the pore water velocity was assumed constant (VK=7.68x10^{-6} cm/sec). Fig. 8 shows the concentration of O_2, NO_3^- and CH_2O at different depths of the column when the pore velocity, VK=7.68x10^{-6} cm/sec and input CH_2O at 6.23 mmol/L in the simulation model. NO_3^- concentration was totally reduced after 2 days at all depths of the column. O_2 and NO_3^- concentration were reduced due to consumption of bacteria X1. Fig. 9 shows the concentration of O_2, NO_3^- and CH_2O at different depths of the column when the pore velocity was increased five times, VK=3.84x10^{-5} cm/sec and the same input CH_2O concentration at 6.23 mmol/L in the simulation model. When pore velocity VK=3.84x10^{-5} cm/sec, NO_3^- concentration decreased after 2 days then increased after 4 days at depths 5 cm and 10 cm of column B. NO_3^- concentration infiltrated down to depth 10 cm due to high pore velocity and lack of CH_2O concentration to reduce NO_3^-.

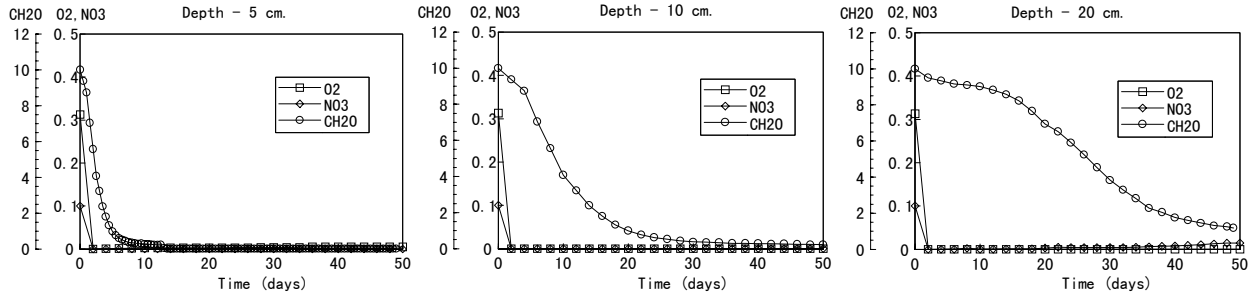

Fig. 8. Mobile redox concentration at different depths with low velocity (VK=7.68x10^{-6} cm/sec)

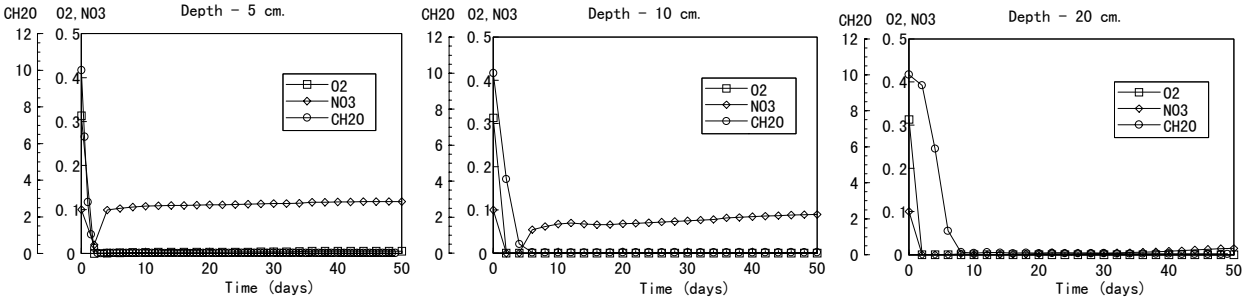

Fig. 9. Mobile redox concentration at different depths with high velocity (VK=3.84x10^{-5} cm/sec)

9.2 Effect of inject CH_2O Concentration

Fig. 10 shows the concentration of O_2, NO_3^- and CH_2O at different depths of the column when the input CH_2O is 0.623 mmol/L and pore velocity VK=7.68x10^{-6} cm/sec. Again NO_3^- concentration decrease after 2 days then increase after 4 days at depths 5 cm and 10 cm of the column. NO_3^- concentration infiltrated deeper down to depth 10 cm due to lack of CH_2O concentration to reduce NO_3^-. Since CH_2O induces denitrification, low concentration of CH_2O will result to NO_3^- infiltration. Fig. 11 shows the concentration of O_2, NO_3^- and CH_2O at different depths of the column when the input CH_2O is 62.3 mmol/L and pore velocity is VK=7.68x10^{-6} cm/sec. NO_3^- concentration was totally reduced at all depths of the column due to sufficient CH_2O concentration. CH_2O

enhanced heterotrophic denitrification, in which bacteria in anaerobic environment uses NO_3^- as electron acceptor to oxidize dissolved CH_2O. CH_2O concentration then increases at depth 20 cm due to lack of O_2. This effect is also dependent on the consumption of bacteria since there is too much CH_2O concentration in excess at this depth.

Table 5 shows the NO_3^- leach at 10 cm depth in relation to input CH_2O concentration and pore velocity *VK*. When VK is $7.68x10^{-6}$ cm/sec and $1.92x10^{-5}$ cm/sec, the plow layer depth at 10 cm is safe for NO_3^- leach. When *VK*=$3.84x10^{-5}$ cm/sec and the input CH_2O concentration is 0.623 mmol/L and 6.23 mmol/L, the plow layer depth at 10 cm is not safe as NO_3^- leach occurred after 4 days. When pore velocity *VK*=$3.84x10^{-5}$ cm/sec, higher concentration of CH_2O at inject water is needed so that NO_3^- leach can be prevented.

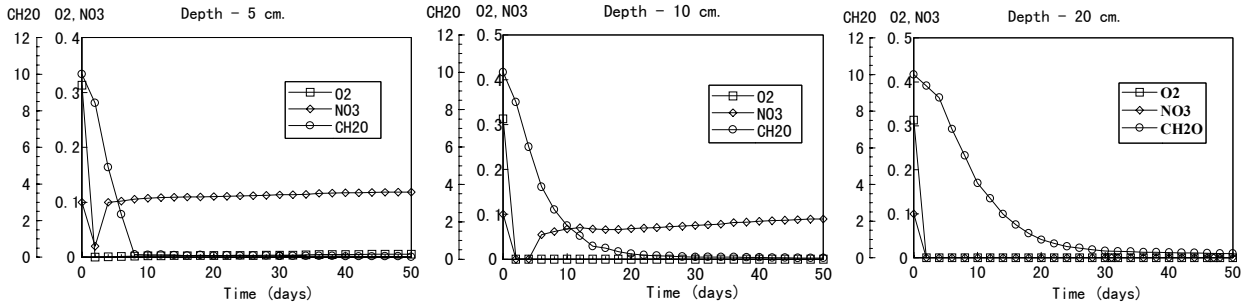

Fig. 10 Mobile redox concentration at different depths with input CH_2O of 62.3 mmol/L and *VK*=$7.68x10^{-6}$ cm/sec

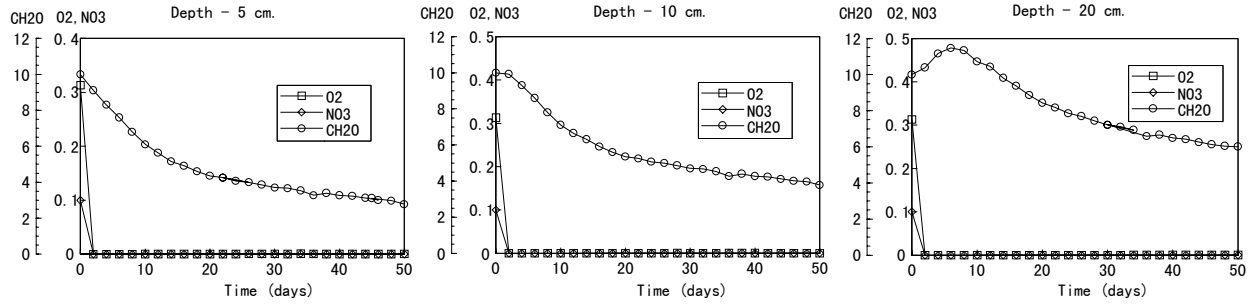

Fig. 11 Mobile redox concentration at different depths with input CH_2O of 62.3 mmol/L and *VK*=$7.68x10^{-6}$ cm/sec

Table 5. NO_3^- leach at 10 cm depth in relation to input CH_2O concentration and pore velocity *VK*

VK /Input CH_2O	CH_2O=0.623 mmol/L	CH_2O=6.23 mmol/L	CH_2O=62.3 mmol/L
VK=$7.68x10^{-6}$ cm/sec	No leach	No leach	No leach
VK=$1.92x10^{-5}$ cm/sec	No leach	No leach	No leach
VK=$3.84x10^{-5}$ cm/sec	NO_3^- LEACH	NO_3^- LEACH	No leach

10 CONCLUSIONS

In designing a wastewater reuse system, it is indispensable to develop an effective treatment scheme that is capable of removing NO_3^- and other contaminants. It is revealed that the multicomponent solute transport model is useful to design the land treatment system for NO_3^- removal from wastewater. CH_2O is a significant quantity because the reduction of NO_3^- and growth of bacteria depend on the presence of CH_2O concentration. When pore velocity *VK*=$7.68x10^{-6}$ cm/sec and *VK*=$1.92x10^{-5}$ cm/sec and input CH_2O concentration are 0.623 mmol/L and 6.23 mmol/, the plow layer at depth 10 cm is still safe as NO_3^- concentration was totally reduced. With pore velocity *VK*=$3.84x10^{-5}$ cm/sec and input CH_2O concentration at 0.623 mmol/L and 6.23 mmol/L, the plow layer

at depth 10 cm is unsafe due to NO_3^- concentration increased again after 4 days. Since CH_2O can enhance denitrification, lack of CH_2O will cause the NO_3^- to increase again. When the pore velocity is high at VK=3.84x10^{-5} cm/sec higher input CH_2O concentration at inject water is needed so that the 10 cm plow layer will be safe. The results show that the multicomponent solute transport model is useful for the description of the biological chemical processes and transport phenomena. Future expansion to two or three dimensions of the model is necessary to address reactive transport at the various scales. Moreover the influence of the change in hydraulic conductivity due to bacterial growth can be very interesting focus of study in the future.

8 REFERENCES

Bear, J. (1972). *Dynamics of Fluid in Porous Media*. Elsevier, New York.

Carrera, J., Vicent, T. and Lafuente, F.J. (2003). "Influence of temperature on denitrification of an industrial high-strength nitrogen wastewater in a two-sludge system." *Water SA*, Vol. 29, pp. 11-16.

Hiroshiro, Y., Jinno, K., Wada, S., Yokoyama, T., and Kubota, M. (1999). "Multicomponent solute transport with cation exchange in a redox subsurface environment. " *ModelCARE99* (Proceedings of the International Conference on Calibration and Reliability in Groundwater Modelling), pp. 474-480.

Kinzelbach, W., Schäfer, W. and Herzer, J. (1991). "Numerical modeling of natural and enhanced denitrification processes in aquifer. " *Water Resources Research*, Vol. 27, No.6, pp. 1149-1159.

Lance, J.C. and Gerba, C.P. (1977). "Nitrogen, phosphate and virus removal from sewage water during land filtration." *Progressive Water Technology*, Vol. 9, pp. 157-166.

Lensing, H.J., Vogt, M. and Herrling, B. (1994). "Modelling of biologically mediated redox processes in the subsurface." *Journal of Hydrology*, Vol. 159, pp. 125-143.

Mac Quarrie, K.T.B. and Sudicky, E.A. (2001). "Multicomponent simulation of wastewater derived nitrogen and carbon in shallow unconfined aquifers I. Model formulation and performance." *Journal of Contaminant Hydrology*, Vol. 47, pp. 53-84.

Mac Quarrie, K.T.B., Sudicky, E.A. and Robertson, W.D. (2001). "Numerical simulation of fine-grained denitrification layer for removing septic system nitrate from shallow groundwater. " *Journal of Contaminant Hydrology*, Vol. 52, pp. 29-55.

Momii K., Hiroshiro Y., Jinno K., Berndtsson, R. (1997). "Reactive solute transport with a variable selectivity coefficient in an undisturbed soil column. " *Soil Science Society of America Journal*, Vol. 61, No.6, pp. 1539-1546.

Postma, D., Boesen, C., Kristiansen, H., and Larsen F. (1991). "Nitrate reduction in an unconfined sandy aquifer: water chemistry, reduction processes and geochemical modeling." *Water Resources Research*, Vol. 27(8), pp. 2027-2045.

Schäfer, D., Schäfer, W. and Kinzelbach W. (1998). "Simulation of reactive processes related to biodegradation in aquifers." *Journal of Contaminant Hydrology*, Vol. 31, No.1, pp.167-209.

Zheng, Z. and Bennet, G.D., (1995). *Applied Contaminant Transport: Modelling, Theory and Practice*. Van Nostrand Reinhold, New York.